J|A|C|S
COMMUNICATIONS

Published on Web 07/21/2007

Bifunctional Anchors Connecting Carbon Nanotubes to Metal Electrodes for Improved Nanoelectronics

Wei-Qiao Deng,[#] Yuki Matsuda, and William A. Goddard III*

Materials and Process Simulation Center, Division of Chemistry and Chemical Engineering, California Institute of Technology, Pasadena, California 91125

Received March 1, 2006; E-mail: wag@wag.caltech.edu

Since their discovery in 1991, carbon nanotubes have attracted much attention due to their unique electric, mechanical, and chemical properties.[1−5] Numerous breakthroughs have led to practical fabrication of carbon nanotube electronics devices, such as transistors,[6] interconnects,[7] spintronics,[8] and sensors. In addition, exfoliated or single graphene sheets show promise as an alternative material for novel electronics devices.[9,10]

Furthermore, a strategy to fabricate a large-scaled carbon nanotube circuit device from single-walled CNTs has been proposed[6,11,12] in which carbon nanotubes are controllably assembled in a specific pattern on the surface and deposited on the metal contacts. Similarly, single graphene sheets are promising for such applications.

Two outstanding obstacles impede this strategy: (1) The carbon nanotubes or graphene sheet may move[13,14] on the contact surface, leading to device unreliability. (2) The contact resistance between the metal contact and a carbon nanotube or graphene sheet can be too high for optimum performance (e.g., 10 MΩ without post-treatment).[15]

To alleviate such problems, we propose connecting the metal contact to the carbon nanotubes via bifunctional molecular anchors. We determine here molecular anchors that would solve these two major problems in CNT and graphene sheet architectures: providing greatly reduced contact resistance (60-fold decrease) and greatly increased mechanical stability.

In order to determine acceptable anchors, we considered the following functional groups, −SH, −OH, $-NH_2$, −COOH, $-CONH_2$, and $-SO_3H$.[16] We assume that the CNT or graphene sheet would be functionalized with a modest coverage (∼1%) of one of these groups. For computational convenience, our model system (Figure 1) has a coverage of ∼8 atom % anchors per surface carbon atoms, a range accessible to experiment.[17] We expect these functional groups to lose hydrogen atoms as they attach to the metal surface, making a strong covalent bond that provides good electrical contact (small contact resistance) between the CNT/graphene and metal while also providing a good mechanical connection (preventing thermal movement of the carbon nanotubes or graphene). To test this concept, we used quantum mechanics (QM using the PBE flavor of density functional theory) to test our designs for molecular anchors by predicting: (1) the structure of the CNT/graphene−anchor−metal interface, (2) interaction *energies* between *anchor and CNT/graphene* and *between anchor and metal*, and (3) the contact resistance between the CNT/graphene and metal for various *anchors*.

To determine the interface structures and anchor energies, we used a 2 × 2 cell of a three-layer Pt(111) slab to describe the Pt surface plus a single graphene sheet to represent the carbon nanotube surface.

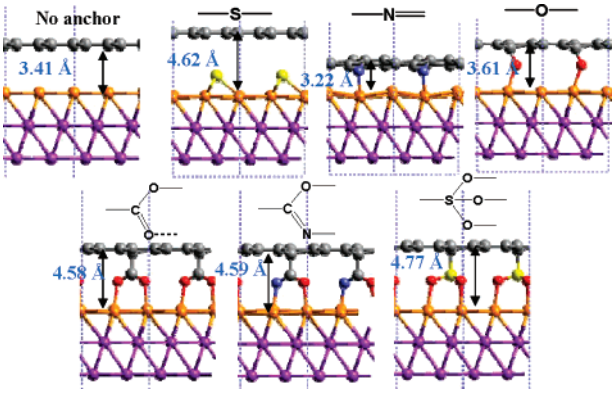

Figure 1. Optimized geometries of various anchors between the Pt(111) surface and the graphene sheet.

We then optimized the structures for the Pt slab−anchor−graphene system with one anchor per cell. (The two bottom layers of Pt atoms were fixed; see Supporting Information.) We find (Table 1 and Figure 1) the (−N−) anchor and the conjugated anchors [(−COO−) and (−CON−)] have the best linkage strengths.

To determine the contact resistance for anchored assemblies, we optimized the sandwich slab structure in Figure 2a. Then we calculated the current/voltage performance (electrical resistance) by combining Green's function theory[17−22] with the DFT Hamiltonian. This leads to

$$I(V) = \frac{2e}{h}\int_{-\infty}^{\infty} T(E,V)[f_1(E,V_1) - f_2(E,V_2)]\mathrm{d}E$$

where $T(E,V)$ is the transmission function of the anchor. The results (Figure 2b) show a contact resistance 60 times lower for the CON anchors and 40 times lower for COO anchors. The results for the contact resistance near zero bias are (in KΩ) −CON− (23.6) < $-SO_3-$ (24.7) < −COO− (37.7) < −O− (49.2) < −N− (54.0) < nonanchor (1480) < −S− (43800).

The very large decrease in contact resistance for (−CON−) and (−COO−) arises partly from their delocalized π-conjugated frontier molecular orbitals that couple well to the conduction orbitals of the electrodes and the graphene. Of course, the σ bonds of the C anchor and Pt anchor also contribute to decreasing the contact resistance, but their role is more important for the bonding. Of course, this effect will not be limited to Pt. We expect similar improvements for other metals such as Pd, Au, Ag, Ni, and Cu. Since the metal−CNT/graphene contact resistance is due to electron transport perpendicular to the interface between the CNT/graphene and electrode surface, we consider that these results for the graphene−metal interface apply equally to the CNT/graphene−metal interface.

[#] Current address: Division of Chemistry and Biological Chemistry, School of Physical & Mathematical Sciences, Nanyang Technological University, Singapore 639798.

10.1021/ja061443r CCC: $37.00

Table 1. Characteristics of Anchored Graphene−Pt(111) Assemblies[a]

	C anchor distance (Å)	C anchor (eV)	Pt anchor distance (Å)	Pt anchor (eV)	linkage strength (eV)	resistance (K ohm)
pure	3.410	**0.0992**			0.0992	1480
−S−	3.545	**0.0002**	1.482	5.87	0.0002	43800
−O−	1.366	2.22	2.055	**0.69**	0.69	49.2
−N−	1.350	6.50	1.979	**2.68**	2.68	54.0
$-SO_3-$	1.858	**0.37**	2.194	1.79	0.37	27.4
−COO−	1.539	**1.84**	2.074	2.18	1.84	37.7
−CON−	1.538	**1.89**	2.051	3.78	1.89	23.6

[a] The linkage strength is the weaker of the two anchor energies (shown in bold). Considering both mechanical stability and contact resistance, the best anchors are (−CON−) and (−COO−).

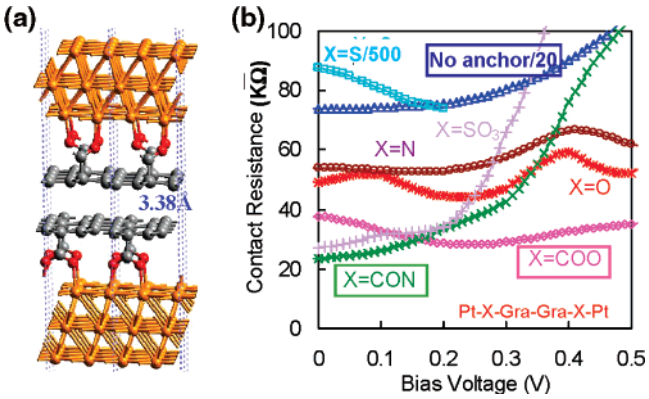

Figure 2. Electrical resistance for current flowing through the Pt−X anchor−graphene−graphene−X anchor−Pt system. The distance between the graphene sheets is 3.38 Å. Here X = −S−, −O−, −N−, −COO−, $-SO_3-$, or − CON−. Note that the No anchor case is scaled by 1/20. Thus the contact resistance for X = −CON− is 60 times lower than that for no anchor, while X = −COO− is 40 times lower.

In the normal configuration for electrodes at two points along the CNT/graphene, there will also be a component of the resistance for electron transport parallel to the CNT/graphene. We consider that this would be small and ignore it. Note that the S anchor leads to a contact resistance even larger than without anchors. This is due to the loss in bonding of S to the graphene, leading to a large tunneling distance.

In conclusion, we find that (−COO−) and (−CON−) bifunctional anchors linking carbon nanotubes or graphene sheets to such metal electrodes as Pt will dramatically improve both the mechanical and electrical properties. This anchor strategy should apply equally to both single-walled and multi-walled nanotubes. It should also improve the properties of metal contacts to graphene, graphite, and carbon black systems.

Such bifunctional anchors are also likely to improve performance of such other CNT/graphene applications as in spintronics (involving linkage to such magnetic metals as Co, Fe, and Ni), but the optimum choices may differ.[8]

In addition to nanoelectronics, we expect that such bifunctional molecular anchors on the surface of carbon supports will lead to improved fuel cell performance by providing reduced internal electrical resistance while impeding catalyst degradation due to aggregation of Pt nanoparticles.[23−25] This should increase the durability of fuel cell catalysts needed to achieve the DOE 2010 goals.

Summarizing, we present the concept of using bifunctional molecular anchors to enhance electrical and mechanical linking of carbon nanotubes to metal electrodes. We show that (−CON−) and (−COO−) anchors are particularly effective for these purposes.

Acknowledgment. We thank Dr. Florian Gstrein, Dr. James M. Blackwell, and Kevin O'Brien (Intel Components Research) for helpful discussions. This research was supported by Intel Components Research with additional partial support provided by NSF-CCF-052-4490, NSF-CTS-054-8774, DARPA-PROM-N00014-02-1-0839, and MARCO-FENA. The facilities of the Materials and Process Simulation Center used for this research are supported by ONR-DURIP, ARO-DURIP, NSF-CCF-052-4490, NSF-CTS-054-8774, DARPA-PROM-N00014-02-1-0839, and MARCO-FENA.

Supporting Information Available: Computational methods and detailed results. This material is available free of charge via the Internet at http://pubs.acs.org.

References

(1) Iijima, S. *Nature* **1991**, *354*, 56−58.
(2) Bethune, D. S.; Kiang, C. H., Devries, M. S.; Gorman, G.; Savoy, R.; Vazquez, J.; Beyers, R. *Nature* **1993**, *363*, 605−607.
(3) Kiang, C. H.; Goddard, W. A., III; Beyers, R.; Salem, J. R.; Bethune, D. S. *J. Phys. Chem.* **1994**, *98*, 6612−6618.
(4) Chen, R. J.; Bangsaruntip, S.; Drouvalakis, K. A.; Kam, N. W. S.; Shim, M.; Li, Y. M.; Kim, W.; Utz, P. J.; Dai, H. J. *Proc. Natl. Acad. Sci. U.S.A.* **2003**, *100*, 4984−4989.
(5) Zhang, Y. G.; Chang, A. L.; Cao, J.; Wang, Q.; Kim, W.; Li, Y. M.; Morris, N.; Yenilmez, E.; Kong, J.; Dai, H. J. *Appl. Phys. Lett.* **2001**, *79*, 3155−3157.
(6) Ziegler, M. M.; Picconatto, C. A.; Ellenbogen, J. C.; Dehon, A.; Wang, D.; Zhong, Z.; Lieber, C. M. *Ann. N.Y. Acad. Sci.* **2003**, *1006*, 312−330.
(7) Baughman, R. H.; Zakhidov, A. A.; de Heer, W. A. *Science* **2002**, *297*, 787−792.
(8) Sahoo, S.; Kontos, T.; Furer, J.; Hoffmann, C.; Graber, M.; Cottet, A.; Schonenberger, C. *Nat. Phys.* **2005**, *1*, 99−102.
(9) Geim, A. K.; Novoselov, K. S. *Nat. Mater.* **2007**, *6*, 183−191 and references therein.
(10) van den Brink, J. *Nat. Nanotechnol.* **2007**, *2*, 199−201 and references therein.
(11) Keren, K.; Berman, R. S.; Buchstab, E.; Sivan, U.; Braun, E. *Science* **2003**, *302*, 1380−1382.
(12) Huang, Y.; Duan, X. F.; Cui, Y.; Lauhon, L. J.; Kim, K. H.; Lieber, C. M. *Science* **2001**, *294*, 1313−1317.
(13) Shirai, Y.; Osgood, A. J.; Zhao, Y. M.; Kelly, K. F.; Tour, J. M. *Nano Lett.* **2005**, *5*, 2330−2334.
(14) Guo, S.; Fogarty, D. P.; Nagel, P. M.; Kandel, S. A. *J. Phys. Chem. B* **2004**, *108*, 14074−14081.
(15) Lee, J. O.; Park, C.; Kim, J. J.; Kim, J.; Park, J. W.; Yoo, K. H. *J. Phys. D: Appl. Phys.* **2000**, *33*, 1953−1956.
(16) Commercialized products see http://www.nanocyl.com/.
(17) Xue, Y. Q.; Datta, S.; Ratner, M. A. *J. Chem. Phys.* **2001**, *115*, 4292−4299.
(18) Seminario, J. M.; Zacarias, A. G.; Derosa, P. A. *J. Phys. Chem. A* **2001**, *105*, 791−795.
(19) Ke, S. H.; Baranger, H. U.; Yang, W. T. *Phys. Rev. B* **2004**, *70*, No. 085410.
(20) Deng, W. Q.; Muller, R. P.; Goddard, W. A., III. *J. Am. Chem. Soc.* **2004**, *126*, 13562−13563.
(21) Kim, Y. H.; Jang, S. S.; Jang, Y. H.; Goddard, W. A., III. *Phys. Rev. Lett.* **2005**, *94*, No. 156801.
(22) Schultz, P. SeqQuest Project; Sandia National Laboratories, Albuquerque, NM, 2003.
(23) Blurton, K. F.; Kunz, H. R.; Rutt, D. R. *Electrochim. Acta* **1978**, *23*, 183−190.
(24) Kazuaki, Y. K.; Taniguchi, A.; Akita, T.; Ioroi, T.; Siroma, Z. *Phys. Chem. Chem. Phys.* **2006**, *8*, 746−752.
(25) Wang, C.; Waje, M.; Wang, X.; Tang, J. M.; Haddon, R. C.; Yan, Y. S. *Nano Lett.* **2004**, *4*, 345−348.

JA061443R